

# Distributed ADMM Approach for the Power Distribution Network Reconfiguration

Yacine Mokhtari, Patrick Coirault, Emmanuel Moulay, Jerome Le Ny and Didier Larraillet

**Abstract**—The electrical network reconfiguration problem aims to minimize losses in a distribution system by adjusting switches while ensuring radial topology. The growing use of renewable energy and the complexity of managing modern power grids make solving the reconfiguration problem crucial. Distributed algorithms help optimize grid configurations, ensuring efficient adaptation to changing conditions and better utilization of renewable energy sources. This paper introduces a distributed algorithm designed to tackle the problem of power distribution network reconfiguration with a radiality constraint. This algorithm relies on ADMM (Alternating Direction Method of Multipliers), where each agent progressively updates its estimation based on the information exchanged with neighboring agents. We show that every agent is required to solve a linearly constrained convex quadratic programming problem and a Minimum Weight Rooted Arborescence Problem (MWRAP) with local weights during each iteration. Through numerical experiments, we demonstrate the performance of the proposed algorithm in various scenarios, including its application to a 33-bus test system and a real-world network.

**Index Terms**—ADMM, minimum spanning tree, arborescence problem, graph theory, mixed-integer non-linear programming (MINLP), optimal network configuration, power loss minimization, radial distribution networks, distributed optimization.

## I. INTRODUCTION

The Power Distribution Network Reconfiguration (PDNR) problem involves strategically modifying the network's topology by opening and closing switches. The primary aim is to optimize system performance by minimizing power losses while ensuring the network maintains its radial structure. Radial distribution systems are preferred due to their lower maintenance requirements and fewer potential failure points compared to alternative network topologies, as indicated in [1].

PDNR methods can be categorized into heuristic [2]–[5], meta-heuristic [6]–[8] and mathematical optimization-based approaches [9]–[11]. Various methods were employed to address the PDNR problem by utilizing centralized methods [12]. These methods gather all network data and transmit it back to the control center to determine the reconfiguration solution. However, this approach is vulnerable to single-point failures

and cyber-attacks. Furthermore, it can be computationally expensive and unsuitable for large-scale systems. An alternative approach is to use distributed (or decentralized) algorithms. In distributed algorithms, computing agents are only required to share limited amounts of information with a specific subset of other agents. This can enhance cybersecurity and reduce the costs associated with the necessary communication infrastructure. Additionally, distributed algorithms demonstrate robustness in the face of individual agent failures and enable the integration of renewable energy into the grid. Moreover, they can execute parallel computations, which positions them as potentially superior to centralized algorithms in terms of solution speed and the maximum problem size they can address [13].

In the context of the distributed approach for the PDNR problem, the multi-agent approach has been suggested in various studies, including [14]–[16]. However, these approaches often require agents, or some of them, to have access to all information, which presents challenges related to data privacy and vulnerability to single-point failures. Moreover, they typically overlook the development of scalable solutions for large-scale distribution networks. Another approach to address the distributed PDNR problem is the Alternating Direction Method of Multipliers (ADMM) used in [17]–[19].

The ADMM algorithm is a primal-dual splitting method initially designed to solve convex optimization problems [20], [21]. ADMM as a general heuristic for solving non-convex problems is mentioned in [20, Ch 9] and this idea is further explored in [22], [23]. Recently, it has garnered attention as a method for discovering approximate solutions for NP-hard problems. Utilizing ADMM for mixed-integer problems offers a significant benefit by requiring only a method to compute the projection onto the discrete constraint set, either exactly or approximately if the computation is costly [22]. While there is no guarantee that ADMM-based methods converge to a global solution for non-convex problems, they are still useful in finding high-quality local solutions.

ADMM algorithm has proven to be a powerful tool for solving the distributed optimal power flow problem by decomposing it into smaller, more manageable subproblems. Studies such as [24], [25], [25] demonstrate ADMM's effectiveness in improving computational efficiency and system resilience without relying on centralized control. Recent works, including [26], [27] further highlight ADMM's role in enhancing the robustness and scalability of power system optimization in distributed and cyber-physical contexts.

Regarding the application of ADMM in PDNR problems, a distributed ADMM-based algorithm was presented in [17].

LIAS (UR 20299), ISAE-ENSMA/Université de Poitiers, 2 rue Pierre Brousse, 86073 Poitiers Cedex 9, France. E-mail: yacine.mokhtari@ensma.fr, patrick.coirault@univ-poitiers.fr

XLIM (UMR CNRS 7252), Université de Poitiers, 11 bd Marie et Pierre Curie, 86073 Poitiers Cedex 9, France. E-mail: emmanuel.moulay@univ-poitiers.fr

Department of Electrical Engineering, Polytechnique Montréal and GERAD, Montreal, QC H3T-1J4, Canada. E-mail: jerome.le-ny@polymtl.ca  
SRD Energies, 78 Av. Jacques Coeur, 86000 Poitiers. E-mail: didier.larraillet@srd-energies.fr

However, it can lead to infeasible solutions due to the lack of a guaranteed radial network structure, as only projections onto the binary set were considered. To address this issue, an enhanced ADMM-based algorithm was proposed in [18]. This algorithm incorporates a proximal operator with a penalty parameter based on residual errors to handle binary variables. Nevertheless, there is still no guarantee of achieving a radial solution since the projection step remains on the binary set. In [19], additional conditions were introduced in the projection step to ensure radiality. The authors combined the algorithms from [17] and [18] with their own, selecting the optimal (feasible) solution among the three. Notably, the examination of radiality constraints on binary variables occurs only after the algorithm's convergence.

The Minimum Spanning Tree (MST) problem is a fundamental challenge in combinatorial optimization, requiring the identification of a tree that spans all vertices in a connected undirected graph while minimizing the total weight of its edges. In the context of directed graphs, the analogous concept to a tree is an arborescence [28], rooted at a specific node, ensuring a directed path from the root to any other node. This problem is known as the Minimum Weight Rooted Arborescence Problem (MWRAP) [28].

Various heuristic algorithms address the PDNR problem by utilizing solutions to the MST problem [2], [29]–[33]. However, these algorithms are centralized and rely on specific assumptions grounded in engineering knowledge of the distribution network. These assumptions include the anticipation that losses are near-optimal when all tie-switches are closed, forming a weakly meshed network. Additionally, they assume a moderate balance in load distribution among feeders and a voltage profile close to the best possible [29].

*Contributions:* This work makes the following contributions:

- We present a distributed ADMM-based algorithm that improves upon the methods introduced in [17]–[19], where relaxation techniques were employed. Unlike these previous approaches, which relax the binary variable, our method utilizes a natural variable substitution. Numerical simulations demonstrate the superiority of our approach compared to the relaxation techniques.
- We demonstrate that the projection step onto the set of radiality constraints in the ADMM algorithm is equivalent to solving an MWRAP. The specific weights in this context are determined by the flow, which is the solution to a linearly constrained convex quadratic programming problem, and the update of the ascent dual variable. This approach differs from previous works [17]–[19], which only project onto the binary set. Such binary projections may result in infeasible solutions.

The article is structured as follows. The proposed mathematical model is presented in Section II. Section III describes the optimization algorithm, and Section IV presents numerical simulation results.

## II. THE OPTIMIZATION PROBLEM FOR THE SIMPLIFIED DISTFLOW MODEL

The structure of the power distribution network can be depicted as a graph containing nodes and connections known as edges (or arcs if a direction is considered). Within this graph, the edges symbolize the electrical lines responsible for carrying power, and the resistivity properties of these lines result in electrical losses, contributing to a specific cost per line. The grid consists of a generator, which holds all the power; source nodes, also known as substations or feeders, which do not hold any power but simply transmit energy to consumer nodes or buses; renewable energy nodes capable of both producing and consuming power; and load buses dedicated solely to power consumption. It is essential to highlight that substations do not receive power from any other nodes except the generator. In our context, the nodes can be simple buses or clusters. We assume that every node in a grid is equipped with a processor capable of making computations as an agent. We also assume that all the lines are switchable.

Let us now introduce some notations that will be useful later. Consider a finite directed strongly connected graph  $G(\mathcal{V}, \mathcal{A})$ , where  $\mathcal{V}$  is the set of nodes and  $\mathcal{A} \subset \mathcal{V} \times \mathcal{V}$  is the set of arcs.  $|\mathcal{V}|$  and  $|\mathcal{A}|$  denote the cardinal of  $\mathcal{V}$  and  $\mathcal{A}$  respectively. An arc going from node  $i$  to node  $j$  is denoted by the ordered pair  $(i, j)$ . We assume that each edge in  $G$  is bidirectional, i.e.,  $(j, i) \in \mathcal{A}$  if  $(i, j) \in \mathcal{A}$ . The generator node is indexed by  $g$ . Let us denote by  $\mathcal{R} \subset \mathcal{V}$  the set of source nodes, assumed connected to  $g$ , and by  $\mathcal{B} := \mathcal{V} \setminus (\mathcal{R} \cup \{g\})$  the set of buses. The Hadamard product, also known as the element-wise product, of the vectors  $\mathbf{x} \in \mathbb{R}^n$  and  $\mathbf{y} \in \mathbb{R}^n$  is defined by:

$$\mathbf{x} \odot \mathbf{y} := (x_1 y_1, \dots, x_n y_n)^T.$$

Bold symbols consistently represent vectors or matrices. If  $\mathbf{x}, \mathbf{y}, \mathbf{z} \in \mathbb{R}^n$  then  $\mathbf{z} \in [\mathbf{x}, \mathbf{y}]$  means that  $z_i \in [x_i, y_i]$  for all  $i \in \{1, \dots, n\}$ . Moreover,  $[\mathbf{x}]_e$  denotes the  $e$ -th element of the vector  $\mathbf{x}$ . The vectors  $\mathbf{0}_n$  and  $\mathbf{1}_n$  denote vectors of size  $n$  consisting entirely of zeros and ones, respectively.

Here, we model EDS by using the *simplified DistFlow model* (SDM) introduced in [4], see also [10, Section III.A] for more details. The formula expressing power loss on the arc connecting nodes  $i$  and  $j$  can be stated as follows [4]:

$$\text{loss}_{ij} = \frac{r_{ij} (P_{ij}^2 + Q_{ij}^2)}{V_i^2}. \quad (1)$$

In this equation,  $r_{ij} > 0$ ,  $P_{ij} \geq 0$  and  $Q_{ij} \geq 0$  correspond to the resistance, active, and reactive power flow through the connection  $(i, j)$ .  $V_i$  denotes the voltage magnitude at the node  $i$ . We assume that the voltage variations along the network must stay within strict regulatory bounds:

$$(1 - \epsilon)^2 \leq \frac{V_i^2}{V_0^2} \leq (1 + \epsilon)^2, \quad \forall i \in \mathcal{V}, \quad (2)$$

where  $V_0$  represents the reference base voltage. In general, we have  $\epsilon \approx 0.05$ , see for instance [4].

According to [4], [10], for each  $(i, j) \in \mathcal{A}$ , the following relation between  $V_i^2$  and  $V_j^2$  holds:

$$V_j^2 = V_i^2 - 2(r_{ij}P_{ij} + x_{ij}Q_{ij}) + (r_{ij}^2 + x_{ij}^2) \frac{P_{ij}^2 + Q_{ij}^2}{V_i^2}, \quad (3)$$

where  $x_{ij} > 0$  is the reactance of the line  $(i, j)$ . We denote:

$$U_i := \frac{V_i^2}{V_0^2}, \quad i \in \mathcal{V},$$

and for the sake of clarity we keep the notation  $r_{ij}$  and  $x_{ij}$  for  $\frac{r_{ij}}{V_0^2}$  and  $\frac{x_{ij}}{V_0^2}$ , respectively. In addition to the above constraints, the forward updates in the buses must be satisfied for each bus  $i \in \mathcal{V}$ :

$$\begin{aligned} \operatorname{div}(\mathbf{P})_i &:= \sum_{j:(i,j) \in \mathcal{A}} P_{ij} - \sum_{j:(j,i) \in \mathcal{A}} P_{ji} \\ &= \rho_i^1 - \sum_{j:(i,j) \in \mathcal{A}} r_{ij} \frac{P_{ij}^2 + Q_{ij}^2}{V_i^2}, \end{aligned} \quad (4)$$

and

$$\begin{aligned} \operatorname{div}(\mathbf{Q})_i &:= \sum_{j:(i,j) \in \mathcal{A}} Q_{ij} - \sum_{j:(j,i) \in \mathcal{A}} Q_{ji} \\ &= \rho_i^2 - \sum_{j:(i,j) \in \mathcal{A}} x_{ij} \frac{P_{ij}^2 + Q_{ij}^2}{V_i^2}, \end{aligned} \quad (5)$$

where  $\rho_i^1 \leq 0$  represents the active power and  $\rho_i^2 \leq 0$  represents the reactive power injected at node  $i \in \mathcal{B}$ , for  $k = 1, 2$ . In the following, we assume that the demand matches the production within the network:

$$\sum_{i \in \mathcal{B}} \rho_i^k = \rho_g^k, \quad k = 1, 2.$$

Additionally, we assume that the power flows  $P_{ij}$  and  $Q_{ij}$  should not exceed the capacities  $\bar{P}_{ij}$  and  $\bar{Q}_{ij}$  of the line, which leads to:

$$0 \leq P_{ij} \leq \bar{P}_{ij}, \quad 0 \leq Q_{ij} \leq \bar{Q}_{ij}.$$

As pointed out in [4], in the SDM approximation the quadratic terms in (3), (4), and (5) can be dropped since they represent the losses on the arcs, and hence they are much smaller than the branch power terms  $\mathbf{P} \in \mathbb{R}^{|\mathcal{A}|}$  and  $\mathbf{Q} \in \mathbb{R}^{|\mathcal{A}|}$ . Furthermore, thanks to (2) and for the sake of convexifying the problem (1), the objective can be approximated at each arc  $(i, j)$  as:

$$\operatorname{loss}_{ij} \approx r_{ij} (P_{ij}^2 + Q_{ij}^2).$$

Now, we introduce binary decision variables  $b_{ij} \in \{0, 1\}$  for each arc  $(i, j) \in \mathcal{A}$ . Setting  $b_{ij} = 1$  indicates power flow from  $i$  to  $j$ , while  $b_{ij} = 0$  indicates no power flow. For a line  $(i, j)$  to remain open, power must flow in only one direction, so only one of  $b_{ij}$  or  $b_{ji}$  can be equal to one. Conversely, setting both  $b_{ij} = b_{ji} = 0$  effectively closes the line  $(i, j)$ . These variables  $b_{ij}$  are also useful in formulating mathematical constraints that enforce a radial (or arborescence) topology rooted at  $g$  for the network, as demonstrated in [10], [11], [34], [35]. However, the explicit form of these constraints is not provided here, as it will not be used in the following discussion.

The reconfiguration problem for the SDM can be written as follows:

$$\min_{(\mathbf{P}, \mathbf{Q}, \mathbf{U}, \mathbf{b}) \in \mathbb{X} \times \mathbb{S}} (\mathbf{r} \odot \mathbf{b})^T (\mathbf{P} \odot \mathbf{P} + \mathbf{Q} \odot \mathbf{Q}), \quad (6a)$$

subject to

$$\operatorname{div}(\mathbf{b} \odot \mathbf{P}) = \boldsymbol{\rho}^1, \quad (6b)$$

$$\operatorname{div}(\mathbf{b} \odot \mathbf{Q}) = \boldsymbol{\rho}^2, \quad (6c)$$

$$\mathbf{b} \odot \mathbf{A} \mathbf{U} = 2\mathbf{b} \odot (\mathbf{r} \odot \mathbf{P} + \mathbf{x} \odot \mathbf{Q}), \quad (6d)$$

where the sets  $\mathbb{X}$  and  $\mathbb{S}$  are given by:

$$\mathbb{X} = [\mathbf{0}_{|\mathcal{A}|}, \bar{\mathbf{P}}] \times [\mathbf{0}_{|\mathcal{A}|}, \bar{\mathbf{Q}}] \times [(1 - \epsilon)^2, (1 + \epsilon)^2]^{|\mathcal{V}|},$$

$$\mathbb{S} = \left\{ \mathbf{b} \in \{0, 1\}^{|\mathcal{A}|} : \mathbf{b} \text{ forms an arborescence rooted at } g \right\},$$

and the matrix  $\mathbf{A} \in \mathbb{R}^{|\mathcal{A}| \times |\mathcal{V}|}$  is defined such that:

$$[\mathbf{A} \mathbf{U}]_e = U_i - U_j, \quad \text{if } e = (i, j) \in \mathcal{A}.$$

Note that a feasible solution  $\mathbf{b}$  to the above problem defines an arborescence  $G_{\mathbf{b}} \subseteq G$  (a directed tree) rooted at  $g$ , whose arcs are the closed switches. The reader can refer to [28, Subsection 2.2] for a detailed definition of an arborescence. Throughout this paper, we assume the feasibility of problem (6), meaning that at least one optimal solution exists.

*Remark 2.1:* The voltage drop constraint (3) has been multiplied component-wise with  $\mathbf{b}$  in (6), making it active solely when  $b_{ij} = 1$ . This is different from the ‘‘big- $M$ ’’ method presented in [10], [36] which includes or excludes these constraints using the inequality:

$$|V_j^2 - (V_i^2 - 2(r_{ij}P_{ij} + x_{ij}Q_{ij}))| \leq (1 - b_{ij})M,$$

for all  $(i, j) \in \mathcal{A}$ , where  $M$  is a sufficiently large parameter. In our case, we have adopted the formulation (6d) to represent the combinatorial problem as an MWRAP as it will be explained later.

#### Distribution of computation tasks among agents

First, we introduce the auxiliary variable  $\mathbf{Y}$  and  $\mathbf{Z}$  such that

$$\mathbf{Y} = \mathbf{P} \odot \mathbf{b}, \quad \mathbf{Z} = \mathbf{Q} \odot \mathbf{b}. \quad (7)$$

The next step is to associate every agent  $i \in \mathcal{V}$  with its objective function  $f_i$  to minimize. We introduce the local variables  $\{\mathbf{X}^i\}_{i \in \mathcal{V}}$  defined by

$$\mathbf{X}^i = (\mathbf{Y}^i, \mathbf{Z}^i, \mathbf{P}^i, \mathbf{Q}^i, \mathbf{U}^i) \in \mathbb{R}^{4|\mathcal{A}| + |\mathcal{V}|}, \quad (8)$$

such that

$$\mathbf{X}^i = \mathbf{X}^j, \quad \forall (i, j) \in \mathcal{A}. \quad (9)$$

Constraint (9) ensures that all agents reach a consensus, meaning they converge to a common limit. We use the notation (8) for the sake of brevity in presenting mathematical expressions and it can be omitted as needed. We associate for each  $\mathbf{X}^i$ ,  $i \in \mathcal{V}$ , a local binary vector  $\mathbf{b}^i$  such that

$$\mathbf{Y}^i = \mathbf{P}^i \odot \mathbf{b}^i, \quad (10)$$

$$\mathbf{Z}^i = \mathbf{Q}^i \odot \mathbf{b}^i, \quad (11)$$

$$\mathbf{b}^i \odot \mathbf{A}^i \mathbf{U}^i = 2(\mathbf{r}^i \odot \mathbf{P}^i + \mathbf{x}^i \odot \mathbf{Q}^i), \quad (12)$$

where  $\mathbf{r}^i, \mathbf{x}^i \in \mathbb{R}^{|\mathcal{A}|}$ , are defined by

$$[\mathbf{r}^i]_e = \begin{cases} [\mathbf{r}]_e & \text{if } e = (i, j) \text{ or } e = (j, i), \\ 0, & \text{otherwise,} \end{cases}$$

$$[\mathbf{x}^i]_e = \begin{cases} [\mathbf{x}]_e & \text{if } e = (i, j) \text{ or } e = (j, i), \\ 0, & \text{otherwise,} \end{cases}$$

and  $\mathbf{A}^i \in \mathbb{R}^{|\mathcal{A}| \times |\mathcal{V}|}$ ,  $i \in \mathcal{V}$ , is defined such that

$$[\mathbf{A}^i \mathbf{U}^i]_e = \begin{cases} U_i^i - U_j^i, & \text{if } e = (i, j), \\ U_j^i - U_i^i, & \text{if } e = (j, i), \\ 0, & \text{otherwise.} \end{cases}$$

This setup ensures that each agent  $i \in \mathcal{V}$  has access only to the components of  $\mathbf{r}$  and  $\mathbf{x}$  related to its neighbor. Additionally, we write the constraints (6c) and (6d) in terms of their respective local variables for every agent  $i \in \mathcal{V}$  as

$$\text{div}(\mathbf{Y}^i)_i = \rho_i^1, \quad (13)$$

$$\text{div}(\mathbf{Z}^i)_i = \rho_i^2, \quad (14)$$

which is equivalent to the formulation  $\text{div}(\mathbf{Y}) = \boldsymbol{\rho}^1$  and  $\text{div}(\mathbf{Z}) = \boldsymbol{\rho}^2$  thanks to the connectedness of the graph.

To distribute the objective function (6a) among the agents, let us consider:

$$\sum_{(i,j) \in \mathcal{A}} (Y_{ij}^2 + Z_{ij}^2) r_{ij} = \sum_{i \in \mathcal{V}} f_i(\mathbf{X}),$$

where  $f_i(\mathbf{X})$  is given by

$$f_i(\mathbf{X}) = \sum_{j:(i,j) \in \mathcal{A}} (Y_{ij}^2 + Z_{ij}^2) r_{ij}.$$

The distributed version of problem (6) writes

$$\begin{aligned} \min_{\mathbf{X}^i \in \mathbb{X}, \mathbf{b}^i \in \mathbb{S}, \forall i \in \mathcal{V}} & \sum_{i \in \mathcal{V}} f_i(\mathbf{X}^i), \\ \text{subject to} & \\ \mathbf{X}^i & \text{ satisfies (9)–(14), } \quad \forall i \in \mathcal{V}. \end{aligned} \quad (15)$$

*Remark 2.2:* We could opt for a relaxation approach similar to that in [17]–[19]. However, as it is shown in Section IV, employing the variable substitutions (7) results in superior algorithm performance compared to relaxation techniques.

*Remark 2.3:* It is important to note that problem (15) is a relaxed version of problem (6), and they are not equivalent. The constraints (9)–(12) do not ensure consensus on the binary vectors, i.e.,  $\mathbf{b}^i = \mathbf{b}^j$ ,  $\forall (i, j) \in \mathcal{A}$ . To show this, let us focus only on (10) since the analysis for (11) and (12) is similar. We have for some  $(i, j) \in \mathcal{A}$  from (10):  $\mathbf{Y}^i = \mathbf{P}^i \odot \mathbf{b}^i$  and  $\mathbf{Y}^j = \mathbf{P}^j \odot \mathbf{b}^j$  and from (9) the consensus constraint  $\mathbf{Y}^i = \mathbf{Y}^j$  and  $\mathbf{P}^i = \mathbf{P}^j$ . Combining the last two equalities yields  $\mathbf{P}^i \odot (\mathbf{b}^i - \mathbf{b}^j) = \mathbf{0}_{|\mathcal{A}|}$ , which does not imply necessarily that  $\mathbf{b}^i = \mathbf{b}^j$  when some components of the flow  $\mathbf{P}^i$  are zeros. However, from an intuitive standpoint, if there is no flow passing through a particular  $(i, j) \in \mathcal{A}$  and all the  $P_{ij}^k = 0$  for every  $k \in \mathcal{V}$ , then the switch  $(i, j)$  would be considered closed. Consequently, we have  $b_{ij}^k = b_{ij}^l$  for all  $k, l \in \mathcal{V}$ . This simplification is aimed at making the combinatorial sub-problem more manageable. As demonstrated in Section IV, this simplification has no impact on the algorithm's performance.

### III. THE OPTIMIZATION ALGORITHM

#### A. Review of the MWRAP

Given a directed graph  $G = (\mathcal{V}, \mathcal{A})$  and a vector of weights  $\{h_{ij}\}_{(i,j) \in \mathcal{A}}$ , the MWRAP consists in finding an arborescence  $(\mathcal{V}, \mathcal{T})$ , with  $\mathcal{T} \subset \mathcal{A}$ , rooted at a designated node in  $G$ , that minimizes the sum of weights  $\sum_{(i,j) \in \mathcal{T}} h_{ij}$ . For more details, we refer the reader to [28, Chapter 6.2]. By definition of the set  $\mathbb{S}$ , the MWRAP can also be formulated as an integer linear programming problem as the following

$$\arg \min_{\mathbf{b} \in \mathbb{S}} \mathbf{h}^T \mathbf{b}, \quad (16)$$

Solving (16) as a linear integer problem in every iteration reduces the effectiveness of ADMM as a heuristic approach to our problem. This is attributed to the prolonged convergence time, particularly evident in large-scale networks. In practical scenarios, the MWRAP can be effectively solved by algorithms like Edmond's algorithm, with a runtime of  $O(|\mathcal{A}| + |\mathcal{V}| \log(|\mathcal{V}|))$ , as showed in [28, Chapter 6.3].

#### B. The proposed algorithm

Let us introduce the auxiliary variable  $\mathbf{k} \in \mathbb{R}^{4|\mathcal{A}| + |\mathcal{V}|}$  such that

$$\mathbf{X}^i = \mathbf{X}^j = \mathbf{k}^{ij}, \quad \forall (i, j) \in \mathcal{A}.$$

By considering these new constraints, the augmented Lagrangian associated with problem (15) reads

$$\begin{aligned} \mathcal{L}_\delta \left( \begin{array}{c} \{\mathbf{X}^i\}, \{\mathbf{b}^i\}, \{\mathbf{k}^{ij}\}, \{\boldsymbol{\alpha}^i\}, \\ \{\boldsymbol{\beta}^i\}, \{\boldsymbol{\gamma}^i\}, \{\mathbf{s}^{ij}\}, \{\mathbf{g}^{ij}\} \end{array} \right) &= \sum_{i \in \mathcal{V}} f_i(\mathbf{X}^i) \\ &+ \frac{\delta}{2} \sum_{i \in \mathcal{V}} H_i(\mathbf{X}^i, \mathbf{b}^i, \delta^{-1} \boldsymbol{\alpha}^i, \delta^{-1} \boldsymbol{\beta}^i, \delta^{-1} \boldsymbol{\gamma}^i) \\ &- 2\delta^{-1} \sum_{i \in \mathcal{V}} \|\boldsymbol{\alpha}^i\|^2 - 2\delta^{-1} \sum_{i \in \mathcal{V}} \|\boldsymbol{\beta}^i\|^2 - 2\delta^{-1} \sum_{i \in \mathcal{V}} \|\boldsymbol{\gamma}^i\|^2 \\ &+ \sum_{(i,j) \in \mathcal{A}} (\mathbf{s}^{ij})^T (\mathbf{X}^i - \mathbf{k}^{ij}) + \sum_{(i,j) \in \mathcal{A}} (\mathbf{g}^{ij})^T (\mathbf{X}^j - \mathbf{k}^{ij}) \\ &+ \frac{\delta}{2} \sum_{(i,j) \in \mathcal{A}} \|\mathbf{X}^i - \mathbf{k}^{ij}\|^2 + \frac{\delta}{2} \sum_{(i,j) \in \mathcal{A}} \|\mathbf{X}^j - \mathbf{k}^{ij}\|^2 \end{aligned}$$

where  $\{\boldsymbol{\alpha}^i\}_{i \in \mathcal{V}}$ ,  $\{\boldsymbol{\beta}^i\}_{i \in \mathcal{V}}$ ,  $\{\boldsymbol{\gamma}^i\}_{i \in \mathcal{V}}$ ,  $\{\mathbf{s}^{ij}\}_{(i,j) \in \mathcal{A}}$ ,  $\{\mathbf{g}^{ij}\}_{(i,j) \in \mathcal{A}}$ , are the Lagrange multipliers and  $H_i$  is given by

$$\begin{aligned} H_i(\mathbf{X}^i, \mathbf{b}^i, \boldsymbol{\alpha}^i, \boldsymbol{\beta}^i, \boldsymbol{\gamma}^i) &= \frac{1}{2} \|\mathbf{P}^i \odot \mathbf{b}^i - \mathbf{Y}^i + \boldsymbol{\alpha}^i\|^2 \\ &+ \frac{1}{2} \|\mathbf{Q}^i \odot \mathbf{b}^i - \mathbf{Z}^i + \boldsymbol{\beta}^i\|^2 \\ &+ \frac{1}{2} \|\mathbf{b}^i \odot \mathbf{A}^i \mathbf{U}^i - 2(\mathbf{r}^i \odot \mathbf{Y}^i + \mathbf{x}^i \odot \mathbf{Z}^i) + \boldsymbol{\gamma}^i\|^2, \end{aligned} \quad (17)$$

The ADMM iterates are given by

$$\begin{aligned} \mathbf{X}_{k+1}^i &\in \arg \min_{\mathbf{X}^i \in \mathbb{X}} \mathcal{L}_\delta \left( \begin{array}{c} \{\mathbf{X}^i\}, \{\mathbf{k}_k^{ij}\}, \{\mathbf{b}_k^i\}, \{\boldsymbol{\alpha}_k^i\}, \\ \{\boldsymbol{\beta}_k^i\}, \{\boldsymbol{\gamma}_k^i\}, \{\mathbf{s}_k^{ij}\}, \{\mathbf{g}_k^{ij}\} \end{array} \right), \\ \mathbf{k}_{k+1}^{ij} &\in \arg \min_{\mathbf{k}^{ij}} \mathcal{L}_\delta \left( \begin{array}{c} \{\mathbf{X}_{k+1}^i\}, \{\mathbf{k}^{ij}\}, \{\mathbf{b}_k^i\}, \{\boldsymbol{\alpha}_k^i\}, \\ \{\boldsymbol{\beta}_k^i\}, \{\boldsymbol{\gamma}_k^i\}, \{\mathbf{s}_k^{ij}\}, \{\mathbf{g}_k^{ij}\} \end{array} \right), \end{aligned}$$

$$\mathbf{b}_{k+1}^i \in \arg \min_{\mathbf{b}^i \in \mathcal{S}} \mathcal{L}_\delta \left( \left\{ \mathbf{X}_{k+1}^i \right\}, \left\{ \mathbf{k}_{k+1}^{ij} \right\}, \left\{ \mathbf{b}^i \right\}, \left\{ \boldsymbol{\alpha}_k^i \right\}, \left\{ \boldsymbol{\beta}_k^i \right\}, \left\{ \boldsymbol{\gamma}_k^i \right\}, \left\{ \mathbf{s}_k^i \right\}, \left\{ \mathbf{g}_k^i \right\} \right),$$

$$\begin{aligned} \boldsymbol{\alpha}_{k+1}^i &= \boldsymbol{\alpha}_k^i + \delta \left( \mathbf{Y}_{k+1}^i - \mathbf{P}_{k+1}^i \odot \mathbf{b}_{k+1}^i \right), \\ \boldsymbol{\beta}_{k+1}^i &= \boldsymbol{\beta}_k^i + \delta \left( \mathbf{Z}_{k+1}^i - \mathbf{Q}_{k+1}^i \odot \mathbf{b}_{k+1}^i \right), \\ \boldsymbol{\gamma}_{k+1}^i &= \boldsymbol{\gamma}_k^i + \delta \left( \begin{array}{c} \mathbf{b}_{k+1}^i \odot \mathbf{A}^i \mathbf{U}_{k+1}^i \\ -2 \left( \mathbf{r}^i \odot \mathbf{Y}_{k+1}^i + \mathbf{x}^i \odot \mathbf{Z}_{k+1}^i \right) \end{array} \right), \\ \mathbf{s}_{k+1}^{ij} &= \mathbf{s}_k^{ij} + \delta \left( \mathbf{X}_{k+1}^i - \mathbf{k}_{k+1}^{ij} \right), \\ \mathbf{g}_{k+1}^{ij} &= \mathbf{g}_k^{ij} + \delta \left( \mathbf{X}_{k+1}^j - \mathbf{k}_{k+1}^{ij} \right). \end{aligned}$$

A closed form can be obtained for  $\mathbf{k}_{k+1}^{ij}$ . Indeed, since the variable  $\mathbf{k}^{ij}$  is unconstrained, we solve  $\nabla_{\mathbf{k}_{k+1}^{ij}} \mathcal{L}_\delta = \mathbf{0}_{|\mathcal{A}|}$  to get

$$\mathbf{0}_{|\mathcal{A}|} = - \left( \mathbf{s}_k^{ij} + \mathbf{g}_k^{ij} \right) + 2\delta \mathbf{k}_{k+1}^{ij} - \delta \mathbf{X}_{k+1}^i - \delta \mathbf{X}_{k+1}^j,$$

that is

$$\mathbf{k}_{k+1}^{ij} = \frac{1}{2\delta} \left( \mathbf{s}_k^{ij} + \mathbf{g}_k^{ij} \right) + \frac{1}{2} \left( \mathbf{X}_{k+1}^i + \mathbf{X}_{k+1}^j \right). \quad (18)$$

Inserting (18) in the dual updates formulas we get

$$\begin{aligned} \mathbf{s}_{k+1}^{ij} &= \frac{1}{2} \left( \mathbf{s}_k^{ij} - \mathbf{g}_k^{ij} \right) + \frac{\delta}{2} \left( \mathbf{X}_{k+1}^i - \mathbf{X}_{k+1}^j \right), \\ \mathbf{g}_{k+1}^{ij} &= \frac{1}{2} \left( \mathbf{g}_k^{ij} - \mathbf{s}_k^{ij} \right) + \frac{\delta}{2} \left( \mathbf{X}_{k+1}^j - \mathbf{X}_{k+1}^i \right). \end{aligned}$$

By taking the sum of the above formulas we obtain  $\mathbf{s}_k^{ij} + \mathbf{g}_k^{ij} = \mathbf{0}_{|\mathcal{A}|}$ ,  $k \geq 1$ , which implies that

$$\mathbf{k}_{k+1}^{ij} = \frac{1}{2} \left( \mathbf{X}_{k+1}^i + \mathbf{X}_{k+1}^j \right). \quad (19)$$

The dual updates become

$$\begin{aligned} \mathbf{s}_{k+1}^{ij} &= \mathbf{s}_k^{ij} + \frac{\delta}{2} \left( \mathbf{X}_{k+1}^i - \mathbf{X}_{k+1}^j \right), \\ \mathbf{g}_{k+1}^{ij} &= \mathbf{g}_k^{ij} + \frac{\delta}{2} \left( \mathbf{X}_{k+1}^j - \mathbf{X}_{k+1}^i \right). \end{aligned}$$

Defining the new multiplier  $\{\boldsymbol{\lambda}_i\}_{i \in \mathcal{V}}$  such that

$$\boldsymbol{\lambda}_{k+1}^i = \sum_{j:(i,j) \in \mathcal{A}} \mathbf{s}_{k+1}^{ij} + \sum_{j:(j,i) \in \mathcal{A}} \mathbf{g}_{k+1}^{ji}, \quad i \in \mathcal{V}, \quad (20)$$

then

$$\boldsymbol{\lambda}_{k+1}^i = \boldsymbol{\lambda}_k^i + \delta \sum_{j \in N(i)} \left( \mathbf{X}_{k+1}^i - \mathbf{X}_{k+1}^j \right), \quad i \in \mathcal{V}.$$

So, the iterate with respect to the variable  $\mathbf{X}_{k+1}^i$  writes

$$\begin{aligned} \mathbf{X}_{k+1}^i &= \arg \min_{\mathbf{X}^i \in \mathcal{X}} \sum_{i \in \mathcal{V}} f_i(\mathbf{X}^i) \\ &+ \frac{\delta}{2} H_i(\mathbf{X}^i, \mathbf{b}_k^i, \delta^{-1} \boldsymbol{\alpha}_k^i, \delta^{-1} \boldsymbol{\beta}_k^i, \delta^{-1} \boldsymbol{\gamma}_k^i) \\ &+ (\mathbf{X}^i)^T \boldsymbol{\lambda}_k^i + \delta \sum_{j \in N(i)} \left\| \mathbf{X}^i - \frac{\mathbf{X}_k^i + \mathbf{X}_k^j}{2} \right\|^2. \end{aligned} \quad (21)$$

Finally, by inserting (20) in (21) and rescaling the dual variables, we get the following ADMM iterates to solve problem (15) for each agent  $i \in \mathcal{V}$ :

$$\begin{aligned} \mathbf{X}_{k+1}^i &\in \arg \min_{\mathbf{X}^i \in \mathcal{X}} \delta^{-1} f_i(\mathbf{X}^i) + H_i(\mathbf{X}^i, \mathbf{b}_k^i, \boldsymbol{\alpha}_k^i, \boldsymbol{\beta}_k^i, \boldsymbol{\gamma}_k^i) \\ &+ (\boldsymbol{\lambda}_k^i)^T \mathbf{X}^i + \sum_{j \in N(i)} \left\| \mathbf{X}^i - \frac{\mathbf{X}_k^i + \mathbf{X}_k^j}{2} \right\|^2 \end{aligned} \quad (22a)$$

$$\mathbf{b}_{k+1}^i \in \arg \min_{\mathbf{b}^i \in \mathcal{S}} H_i(\mathbf{X}_{k+1}^i, \mathbf{b}^i, \boldsymbol{\alpha}_k^i, \boldsymbol{\beta}_k^i, \boldsymbol{\gamma}_k^i), \quad (22b)$$

$$\boldsymbol{\alpha}_{k+1}^i = \boldsymbol{\alpha}_k^i + \mathbf{P}_{k+1}^i \odot \mathbf{b}_{k+1}^i - \mathbf{Y}_{k+1}^i, \quad (22c)$$

$$\boldsymbol{\beta}_{k+1}^i = \boldsymbol{\beta}_k^i + \mathbf{Q}_{k+1}^i \odot \mathbf{b}_{k+1}^i - \mathbf{Z}_{k+1}^i, \quad (22d)$$

$$\begin{aligned} \boldsymbol{\gamma}_{k+1}^i &= \boldsymbol{\gamma}_k^i + \mathbf{b}_{k+1}^i \odot \mathbf{A}^i \mathbf{U}_{k+1}^i \\ &- 2 \left( \mathbf{r}^i \odot \mathbf{Y}_{k+1}^i + \mathbf{x}^i \odot \mathbf{Z}_{k+1}^i \right), \end{aligned} \quad (22e)$$

$$\boldsymbol{\lambda}_{k+1}^i = \boldsymbol{\lambda}_k^i + \sum_{j \in N(i)} \left( \mathbf{X}_{k+1}^i - \mathbf{X}_{k+1}^j \right), \quad (22f)$$

where  $N(i)$  is the neighbors set of the agent  $i$ , and  $\delta > 0$  is a quadratic penalty parameter. Iterates (22a) and (22b) are known as the primal updates while iterates (22c)–(22f) are known as the dual ones. Note that the iterates (22a)–(22f) are distributed, namely, each agent  $i$  exclusively exchanges information with its neighboring agents.

It can be seen that problem (22a) is a linearly constrained convex quadratic problem that can be solved by using optimization solvers, while problem (22b) for  $\mathbf{b}^i$ ,  $i \in \mathcal{V}$ , is a mixed-integer quadratic problem that is generally costly to solve. In the Next, we show that it can be seen as an MWRAP with specific local weights.

*Proposition 3.1:* For each  $i \in \mathcal{V}$ , solving problem (22b) is equivalent to solve the MWRAP on  $G$  rooted at  $g$  with weights

$$\begin{aligned} \mathbf{h}^i &= \mathbf{h}_1^i + \mathbf{h}_2^i + \mathbf{h}_3^i \\ &= \mathbf{P}_{k+1}^i \odot \left( \mathbf{P}_{k+1}^i + 2 \left( \boldsymbol{\alpha}_k^i - \mathbf{Y}_{k+1}^i \right) \right) \\ &+ \mathbf{Q}_{k+1}^i \odot \left( \mathbf{Q}_{k+1}^i + 2 \left( \boldsymbol{\beta}_k^i - \mathbf{Z}_{k+1}^i \right) \right) \\ &+ \mathbf{A}^i \mathbf{U}_{k+1}^i \odot \left( \begin{array}{c} \mathbf{A}^i \mathbf{U}_{k+1}^i + 2 \boldsymbol{\gamma}_k^i \\ -4 \left( \mathbf{r}^i \odot \mathbf{Y}_{k+1}^i + \mathbf{x}^i \odot \mathbf{Z}_{k+1}^i \right) \end{array} \right). \end{aligned} \quad (23)$$

**Proof.** By expending the first term of  $H_i(\mathbf{X}_{k+1}^i, \mathbf{b}^i, \boldsymbol{\alpha}_k^i, \boldsymbol{\beta}_k^i, \boldsymbol{\gamma}_k^i)$  we get

$$\begin{aligned} &\left\| \mathbf{P}_{k+1}^i \odot \mathbf{b}^i - \mathbf{Y}_{k+1}^i + \boldsymbol{\alpha}_k^i \right\|^2 \\ &= \left\| \mathbf{P}_{k+1}^i \odot \mathbf{b}^i \right\|^2 + 2 \left( \mathbf{P}_{k+1}^i \odot \mathbf{b}^i \right)^T \left( \boldsymbol{\alpha}_k^i - \mathbf{Y}_{k+1}^i \right) \\ &+ \left\| \boldsymbol{\alpha}_k^i - \mathbf{Y}_{k+1}^i \right\|^2 \\ &= \left( \mathbf{P}_{k+1}^i \odot \mathbf{P}_{k+1}^i \right)^T \mathbf{b}^i + 2 \left( \mathbf{P}_{k+1}^i \odot \left( \boldsymbol{\alpha}_k^i - \mathbf{Y}_{k+1}^i \right) \right)^T \mathbf{b}^i \\ &+ \left\| \boldsymbol{\alpha}_k^i - \mathbf{Y}_{k+1}^i \right\|^2 \\ &= \left( \mathbf{h}_1^i \right)^T \mathbf{b}^i + \left\| \boldsymbol{\alpha}_k^i - \mathbf{Y}_{k+1}^i \right\|^2. \end{aligned} \quad (24)$$

Similarly, by expending the second term of  $H_i(\mathbf{X}_{k+1}^i, \mathbf{b}^i, \boldsymbol{\alpha}_k^i, \boldsymbol{\beta}_k^i, \boldsymbol{\gamma}_k^i)$  We obtain

$$\left\| \mathbf{Q}_{k+1}^i \odot \mathbf{b}^i - \mathbf{Z}_{k+1}^i + \boldsymbol{\beta}_k^i \right\|^2 = \left( \mathbf{h}_2^i \right)^T \mathbf{b}^i + \left\| \boldsymbol{\beta}_k^i - \mathbf{Z}_{k+1}^i \right\|^2 \quad (25)$$

For the third term, we have

$$\begin{aligned}
& \left\| \begin{matrix} \mathbf{b}^i \odot \mathbf{A}^i \mathbf{U}_{k+1}^i + \gamma_k^i \\ -2(\mathbf{r}^i \odot \mathbf{Y}_{k+1}^i + \mathbf{x}^i \odot \mathbf{Z}_{k+1}^i) \end{matrix} \right\|^2 \\
= & \left\| \mathbf{b}^i \odot \mathbf{A}^i \mathbf{U}_{k+1}^i \right\|^2 \\
& + \left\| \gamma_k^i - 2(\mathbf{r}^i \odot \mathbf{Y}_{k+1}^i + \mathbf{x}^i \odot \mathbf{Z}_{k+1}^i) \right\|^2 \\
& + 2(\mathbf{b}^i \odot \mathbf{A}^i \mathbf{U}_{k+1}^i)^T \left( \gamma_k^i - 2 \begin{pmatrix} \mathbf{r}^i \odot \mathbf{Y}_{k+1}^i \\ + \mathbf{x}^i \odot \mathbf{Z}_{k+1}^i \end{pmatrix} \right) \\
= & \left( \begin{matrix} \mathbf{A}^i \mathbf{U}_{k+1}^i \odot \mathbf{A}^i \mathbf{U}_{k+1}^i + \\ 2\mathbf{A}^i \mathbf{U}_{k+1}^i \odot \left( \gamma_k^i - 2 \begin{pmatrix} \mathbf{r}^i \odot \mathbf{Y}_{k+1}^i \\ + \mathbf{x}^i \odot \mathbf{Z}_{k+1}^i \end{pmatrix} \right) \end{matrix} \right)^T \mathbf{b}^i \\
& + \left\| \gamma_k^i - 2(\mathbf{r}^i \odot \mathbf{Z}_{k+1}^i + \mathbf{x}^i \odot \mathbf{Z}_{k+1}^i) \right\|^2 \\
= & (\mathbf{h}_3^i)^T \mathbf{b}^i + \left\| \gamma_k^i - 2(\mathbf{r}^i \odot \mathbf{Z}_{k+1}^i + \mathbf{x}^i \odot \mathbf{Z}_{k+1}^i) \right\|^2
\end{aligned} \tag{26}$$

Above, we have used the fact that  $\mathbf{b}^i \odot \mathbf{b}^i = \mathbf{b}^i$  for  $\mathbf{b}^i \in \mathbb{S}$ . By combining (24)–(26) we get (23). ■

So, at each iteration, each agent represented by  $i \in \mathcal{V}$  is assigned the task of solving both the linearly constrained quadratic problem (22a) and a MWRAP with weights  $\mathbf{h}^i$ . The time complexity of the algorithm in each iteration is primarily determined by the quadratic problem since Edmond’s algorithm has a lower time complexity in comparison.

*Remark 3.2:* We could solve problem (22a) as a linearly constrained quadratic programming problem incorporating constraint (12), thereby eliminating the need for the update with respect to  $\gamma_k^i$  in (22e). However, this approach might render problem (22a) infeasible for certain values of  $k$ , causing the iteration to halt. By separating (22e) from the constrained quadratic programming problem (22a), we can avoid this issue.

Let  $\eta > 0$  and  $k_{\max}$  be an error tolerance parameter and the maximum number of iterations respectively. Let  $e_k, k \geq 0$ , be the successive change in the iterates (22a)–(22f), defined by

$$e_k = \sum_{i \in \mathcal{V}} \left( s_k^i + r_k^i + \sum_{j \in \mathcal{N}(i)} \left\| \mathbf{b}_k^i - \mathbf{b}_k^j \right\| \right), \tag{27}$$

where  $s_k^i$  and  $r_k^i$  are defined by

$$\begin{aligned}
s_k^i & := \left\| (\mathbf{X}, \mathbf{b})_{k+1}^i - (\mathbf{X}, \mathbf{b})_k^i \right\|, \\
r_k^i & := \left\| (\boldsymbol{\alpha}, \boldsymbol{\beta}, \boldsymbol{\gamma}, \boldsymbol{\lambda})_{k+1}^i - (\boldsymbol{\alpha}, \boldsymbol{\beta}, \boldsymbol{\gamma}, \boldsymbol{\lambda})_k^i \right\|.
\end{aligned}$$

The term  $\sum_{j \in \mathcal{N}(i)} \left\| \mathbf{b}_k^i - \mathbf{b}_k^j \right\|$  has been added (27) to guarantee the convergence of the local variables  $\mathbf{b}^i, i \in \mathcal{V}$ , to the same limit  $\mathbf{b}$  (consensus) as there is no guarantee of its occurrence, see Remark 2.3. Our algorithm is stated as follows:

---

### Algorithm 1 Distributed Algorithm

---

**Require:**  $\rho^1, \rho^2, \mathbf{r}, \mathbf{x}, \delta > 0, \eta > 0$ .

- 1: Initialize  $\mathbf{X}_0^i = \boldsymbol{\lambda}_0^i = \mathbf{0}_{4|\mathcal{A}|+|\mathcal{V}|}, \boldsymbol{\alpha}_0^i = \boldsymbol{\beta}_0^i = \boldsymbol{\gamma}_0^i = \mathbf{0}_{|\mathcal{A}|}, \mathbf{b}_0^i = \mathbf{b}_0 \sim \mathcal{N}(0, \sigma \mathbf{I}_{|\mathcal{A}|}), \forall i \in \mathcal{V}, k = 0$ .
  - 2: **repeat**
  - 3:   **for** each agent  $i \in \mathcal{V}$  **do**
  - 4:     Update  $\mathbf{X}_{k+1}^i$  according to (22a).
  - 5:     Update  $\mathbf{b}_{k+1}^i$  according to (22b).
  - 6:     Update  $\boldsymbol{\alpha}_{k+1}^i, \boldsymbol{\beta}_{k+1}^i, \boldsymbol{\gamma}_{k+1}^i, \boldsymbol{\lambda}_{k+1}^i$  according to (22c)–(22f).
  - 7:      $k \leftarrow k + 1$ .
  - 8:   **end for**
  - 9: **until**  $e_k < \eta$  or  $k \geq k_{\max}$
- 

Since the convergence of  $e_k$  to zero in Algorithm 1 is not guaranteed, we increase the likelihood of convergence by running this algorithm multiple times with different initial conditions  $\mathbf{b}_0$ .

*Remark 3.3:* Examining the convergence of the proposed algorithm is a challenging task that falls outside the purview of this paper due to the mixed-integer nature of the problem. Instead, in the following section, we conduct various experiments to showcase both the effectiveness and limitations of our algorithms. It’s crucial to emphasize that in the realm of non-convex optimization problems, ADMM does not assure of attaining an optimal, satisfactory, or even feasible solution within a finite number of iterations [22]. Additionally, it is noteworthy that ADMM’s performance is contingent on the choice of initialization  $\mathbf{b}^0$  and penalty parameter  $\delta$ , unlike the convex case where ADMM converges to an optimal solution regardless of the chosen  $\mathbf{b}^0$  and  $\delta$ .

## IV. NUMERICAL EXPERIMENTS

In this section, we demonstrate the efficiency and limitations of our algorithm through various simulations across different scenarios. The section is structured into three subsections. The first subsection examines a simplified network consisting of five nodes, highlighting the resilience of Algorithm 1 under various conditions. We show that our algorithm converges toward the optimal radial solution although the system changes. In the second subsection, Algorithm 1 is implemented on the 33-bus system [4]. We demonstrate the algorithm’s robustness by showcasing its ability to converge despite encountering a line fault during execution. Additionally, we perform a comparative analysis between our algorithm, its centralized counterpart, and the distributed algorithms presented in [17], [18], as well as their enhanced version that will be proposed later. Our findings demonstrate that Algorithm 1 outperforms all others in terms of performance. The final subsection applies Algorithm 1 to a large-scale network operated by SRD, a French transmission system operator.

Unless there is a change, the tolerance parameter  $\varepsilon$  for the error  $e_k$  defined in (27) and the penalization parameter  $\delta$  are fixed at  $10^{-4} \times |\mathcal{V}|$  and 1 respectively. The Matlab function `quadprog` was used to solve problem (22a) Moreover, the MRSAP is solved by implementing Edmonds’ algorithm in Matlab taken from [37].

### A. Resilience: a toy network

In this subsection, we demonstrate that Algorithm 1 possesses the capability to adapt to dynamic changes within the network environment as they occur in real-time. These adaptations include the detection of modifications such as integrating a new source of energy, switches going offline, or shifts in network traffic patterns. The algorithm subsequently reconfigures the network in response to these changes during its execution without restarting. This process is illustrated in a simple example by considering a graph with a size of  $|\mathcal{V}| = 5$  and one substation indexed by 1. The voltage constraint (3) with their corresponding dual updates are dropped. We set  $c_{ij} = i + j$ , for all  $(i, j) \in \mathcal{A}$ . Our experience is divided into four phases:

- **from  $k = 1$  to  $k = 100$ :** Algorithm 1 is executed with  $\rho^1 = \rho^2 = (4, -1, -1, -1, -1)^T$ . It converges to the optimal solution illustrated in Figure 1a.
- **from  $k = 100$  to  $k = 200$ :** In order to model the failure of the line (2,1) between the 100th and 200th iteration, we assign zero values at each iteration to  $b_{2,1}^1$ ,  $b_{1,2}^1$ ,  $b_{1,2}^2$ , and  $b_{2,1}^2$  so that this modification is known only to agents  $i = 1, 2$ . Algorithm 1 is capable of detecting these line failures and adapting accordingly, ultimately converging to the optimal solution shown in Figure 1b.
- **from  $k = 200$  to  $k = 300$ :** In this phase, we alter the supply-demand vector to  $\rho = (4, -1, -2, 2, -3)^T$  to reflect an increased demand for buses 3 and 5, which is compensated by the renewable energy supplied by node 4. The algorithm seamlessly adapts to these modifications, ultimately converging to the optimal solution within this specific context shown in Figure 1c.
- **from  $k = 300$  to convergence:** During this phase, we assume that the connection between points (1,2) has been restored. Consequently, Algorithm 1 requires modification to ensure it converges towards the optimal solution while adhering to the radiality constraints. These adjustments result in the optimal solution depicted in Figure 1d.

This experience showcases the effectiveness and adaptability of our algorithm in responding to real-time fluctuations, ensuring convergence to a radial solution. The iterative process's evolution, along with multiple quantities during different phases, is illustrated in Figures 2a-2b.

### B. Baran and Wu test case

Algorithm 1 has been tested on the Baran and Wu test case [4] which comprises 33 nodes, 32 branches, and 5 tie lines, with a total active and reactive demand equal to 3.715 MW and 2.24 MVar, respectively, and voltage base 12.66 kV, and a single substation indexed by 1 linked to a generator, as illustrated in Figure 3. The data of the network can be found in [4]. The optimization process involves comparing the outcome of Algorithm 1 with an initial configuration defined by the inactivation of the following lines: (25, 29), (18, 33), (9, 15), (8, 21), (12, 22) resulting in a total approximate loss of 183.74 kW (against 202.7 kW by using the non-simplified model [9]).

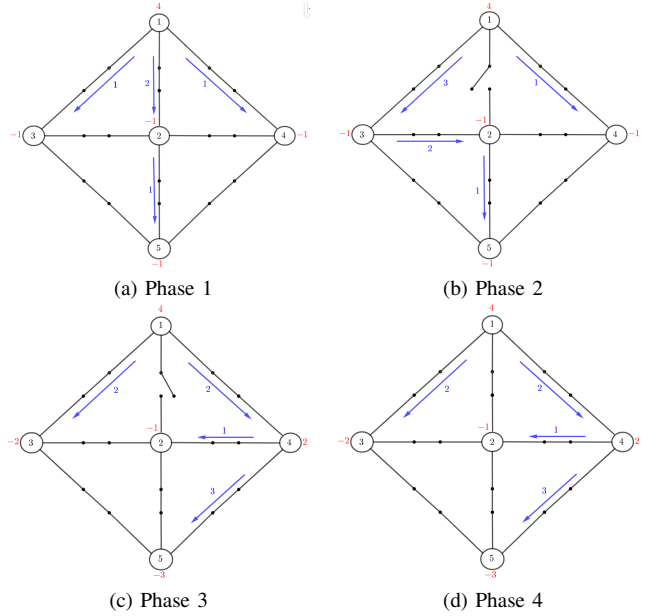


Fig. 1: The various phases of the experience. The supply-demand of nodes and the flow direction are highlighted in red and blue, respectively.

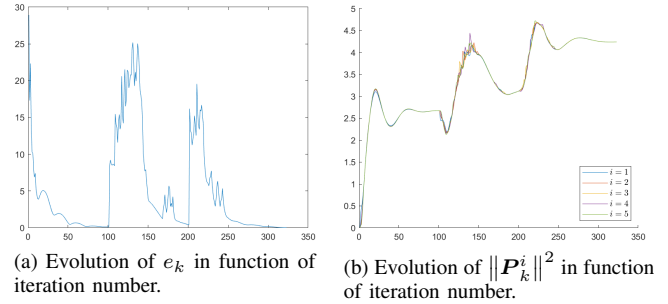


Fig. 2: The various plots show the evolution of different parameters in function of iteration number.

1) *Convergence:* As Algorithm 1 is highly influenced by its initial conditions, it underwent ten executions, each with a distinct  $b_0$ . Among these runs, it effectively determined the best solution, activating switches (8, 21), (9, 10), (14, 15), (28, 29), and (32, 33). This resulted in a loss of 132.28 kW (against 139.5 kW by using the non-simplified model [9]), with  $\delta$  set at 0.1. Achieving this outcome required 1349 iterations, see Figure 4a. Notably, this optimal configuration was attained in only 2 of the 10 restarts. In the remaining runs, Algorithm 1 converged but without reaching the optimal solution. See Table I for more details. We chose the  $\delta$  value in this specific manner to increase the system's sensitivity to cost considerations over the quadratic penalization. It is essential to recognize, however, that increasing the value of  $\delta$  can potentially sacrifice optimality while simultaneously reducing the number of iterations.

2) *Resilience:* We demonstrate the resilience of Algorithm 1 by introducing a fault in the line (17, 18) (any other line can be chosen) after the 1200th iteration. This is done by setting  $b_{(17,18)}^{17} = b_{(18,17)}^{17} = b_{(17,18)}^{18} = b_{(18,17)}^{18} = 0$ ,

TABLE I: Execution results of Algorithm 1 on the 33-bus system for various  $\delta$  values. Averages are computed over 10 runs.

	Average Losses (kW)	Min-Max Losses (kW)	Average No. of Iterations	Feasibility Ratio
$\delta = 0.1$	140.1	132.28-143.11	1430	10/10
$\delta = 1$	156.43	143.76-163.18	1190	10/10
$\delta = 10$	172.3	162.9-180.2	871	10/10
$\delta = 100$	188.4	176.08-198.55	517	10/10
$\delta = 10^8$	201.76	190.65-212.62	497	10/10

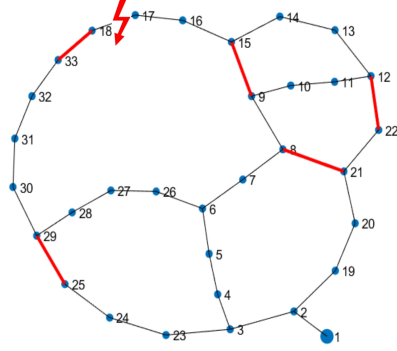
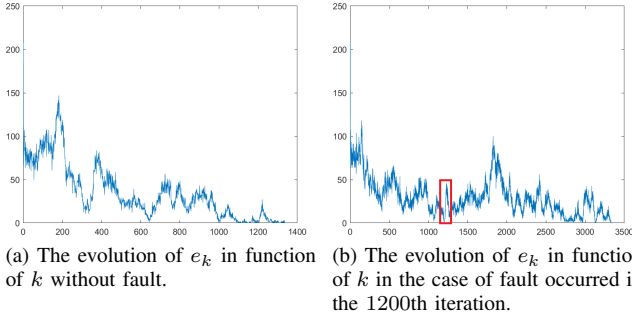


Fig. 3: Baran and Wu network. The lines in red are inactive in the initial configuration. The Fault occurs in the line (17, 18) after the 1200th iteration.



(a) The evolution of  $e_k$  in function of  $k$  without fault. (b) The evolution of  $e_k$  in function of  $k$  in the case of fault occurred in the 1200th iteration.

Fig. 4: The evolution of  $e_k$  as a function of  $k$  in scenarios with and without a fault.

ensuring that the fault is only known locally to agents 17 and 18. Under these conditions, Algorithm 1 required 3352 iterations to converge to the solution with open switches at (7, 8), (10, 11), (14, 15), (17, 18), and (28, 29), resulting in a loss of 157.8 kW. The progression of the error  $e_k$  is illustrated in Figure 4b.

### C. Centralized vs distributed

In this section, we compare Algorithm 1 with its centralized counterpart, which involves the following iterations:

$$\begin{aligned}
 \mathbf{X}^{k+1} &\in \arg \min_{\mathbf{X} \in \mathbb{X}} \delta^{-1} \mathbf{r}^T (\mathbf{Y} \odot \mathbf{Y} + \mathbf{Z} \odot \mathbf{Z}) \\
 &\quad + H(\mathbf{X}, \mathbf{b}_k, \boldsymbol{\alpha}_k, \boldsymbol{\beta}_k, \boldsymbol{\lambda}_k), \\
 \mathbf{b}^{k+1} &\in \arg \min_{\mathbf{b} \in \mathbb{S}} H(\mathbf{X}_{k+1}, \mathbf{b}, \boldsymbol{\alpha}_k, \boldsymbol{\beta}_k, \boldsymbol{\lambda}_k), \\
 \boldsymbol{\alpha}^{k+1} &= \boldsymbol{\alpha}^k + \mathbf{P}^{k+1} \odot \mathbf{b}^{k+1} - \mathbf{Y}^{k+1}, \\
 \boldsymbol{\beta}^{k+1} &= \boldsymbol{\beta}^k + \mathbf{Q}^{k+1} \odot \mathbf{b}^{k+1} - \mathbf{Z}^{k+1}, \\
 \boldsymbol{\lambda}^{k+1} &= \boldsymbol{\lambda}^k + \mathbf{b} \odot \mathbf{A} \mathbf{U}_{k+1} \\
 &\quad - 2(\mathbf{r} \odot \mathbf{Y}_{k+1} + \mathbf{x} \odot \mathbf{Z}_{k+1})
 \end{aligned}$$

In this context, all vectors are defined similarly but without the agent's indices  $i \in \mathcal{V}$ . Similar to Proposition 3.1, we can show that the problem for  $\mathbf{b}$  is an MWRSA problem with the same weights, excluding the agents' indices. For the centralized algorithm, we fix the error tolerance parameter at  $10^{-4}$ .

Table II presents the results of the centralized algorithm on the 33-bus system. As indicated in Table I, the distributed algorithm requires significantly more iterations to reach convergence compared to the centralized version. This is due to the distributed approach's limitation, where agents only have information about their neighboring nodes.

The centralized algorithm consistently achieves lower average losses compared to the distributed algorithm and exhibits more consistent performance with narrower min-max loss ranges. It requires fewer iterations and has shorter overall computation times compared to the global convergence time of the distributed algorithm. Specifically, the centralized algorithm takes 8.27 seconds on average, whereas the distributed algorithm takes 61.3 seconds for all 33 agents, or approximately 1.86 seconds per agent. Both algorithms maintain a perfect feasibility ratio. While the centralized algorithm provides more optimal and efficient solutions, the distributed algorithm has a shorter computation time per agent.

1) *Algorithm 1 Compared to [17] and [18]*: In this section, we compare Algorithm 1 with those proposed in [17] and [18], where a relaxation technique is used instead of the variable substitution (7). The combinatorial problem with respect to  $\mathbf{b}^i$  for  $i \in \mathcal{V}$  is defined as:

$$\mathbf{b}^i = \arg \min_{\mathbf{b}^i \in \mathbb{S}} \|\mathbf{w}_{k+1}^i - \mathbf{b}^i + \mathbf{u}_k^i\|, \quad (28)$$

where  $\mathbf{w}^i \in [0, 1]^{|A|}$  is the relaxation of  $\mathbf{b}^i$  and  $\mathbf{u}^i$  is the Lagrange multiplier for the constraints  $\mathbf{w}^i = \mathbf{b}^i$ ,  $i \in \mathcal{V}$ . The improvement of [18] over [17] lies in the level of the projection operator where the Douglas-Rachford splitting method was used. However, in both papers, problem (28) is treated as a



TABLE II: Results for centralized algorithm on the 33-bus system with different values of  $\delta$ .

	Average Losses (kW)	Min-Max Losses (kW)	Average No. of Iterations	Average Time (s)	Feasibility Ratio
$\delta = 1$	137.8	132.09-140.87	146	8.27	10/10
$\delta = 10$	152.3	146.7-158.4	31	1.12	10/10
$\delta = 100$	166.8	152.12-188.7	14	0.32	10/10
$\delta = 10^8$	198.2	175.2-224	4	0.09	10/10

projection problem of  $\mathbf{w}_{k+1}^i + \mathbf{u}_k^i$  onto the set  $\{0, 1\}^{|\mathcal{A}|}$ , which does not ensure the tree structure of the solution. Instead, in the same spirit of Proposition 3.1, it can be shown that problem (28) can be solved by solving an MWRAP with weights:

$$\mathbf{h}^i = -\mathbf{w}_{k+1}^i - \mathbf{u}_k^i, \quad i \in \mathcal{V}. \quad (29)$$

We refer to the algorithm from [17] and [18], which handles problem (28) by solving the MWRAP with weights, as "Algorithm *relax*". Unfortunately, the algorithm from [19] cannot be included in the comparison process since no explicit formula for the projection operator was provided. As before, we run Algorithm 1, Algorithm *relax*, and the algorithms from [17] and [18] 10 times with different  $\mathbf{b}_0$  then we take the average of these runs.

TABLE III: Iteration counts and feasibility ratio over 10 runs of Algorithm 1, Algorithm *relax*, and the algorithms from [17] and [18].

⊠ : heuristic did not converge after  $k_{\max} = 5000$ .  
\* : the solution is not radial.

	Algorithm 1	Algorithm <i>relax</i>	[17]	[18]
$\delta = 0.1$	1430 - 10/10	⊠	⊠	⊠
$\delta = 1$	1190 - 10/10	4761 - 6/10	⊠	⊠
$\delta = 10$	871 - 10/10	3981 - 8/10	⊠	*
$\delta = 100$	517 - 10/10	3560 - 8/10	*	*
$\delta = 10^8$	497 - 10/10	2912 - 9/10	*	*

Table III summarizes the performance of the various algorithms across different values of  $\delta$ , with each algorithm executed ten times. Several key observations can be drawn from this comparison:

Algorithm 1 consistently converges in all runs across different  $\delta$  values, demonstrating robust performance with iteration counts decreasing as  $\delta$  increases. In contrast, Algorithm *relax* shows mixed results. It fails to converge for  $\delta = 0.1, 1$ , and 10. For higher values of  $\delta$ , it converges in fewer iterations but less consistently than Algorithm 1. The algorithms from [17] and [18] mostly fail to converge, especially for lower values of  $\delta$ . When they do converge, the solutions are not radial.

For higher values of  $\delta$  ( $\delta = 10^8$ ), both Algorithm *relax* and the referenced algorithms show improved feasibility ratios, but still not as high as Algorithm 1. This comparison indicates that Algorithm 1 is superior in terms of consistency and iteration efficiency across different values of  $\delta$ . The use of a relaxation technique in Algorithm *relax* and the methods from [17] and [18] appears less reliable than the variable substitution (7), particularly for lower  $\delta$  values.

#### D. Real case study

We conducted experiments on a real-world power grid managed by SRD, which supplied the necessary data. This

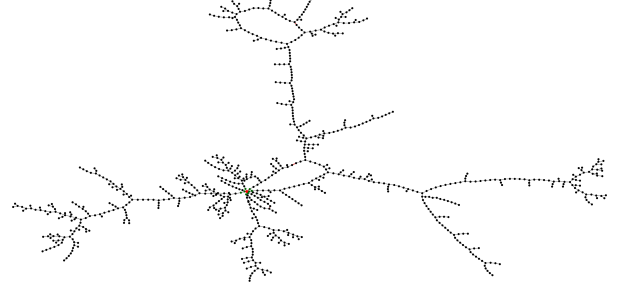


Fig. 5: The SRD power grid. The big red node in the center of the network represents the generator, the green nodes denote the substations. The red lines are the open switches in the optimal case.

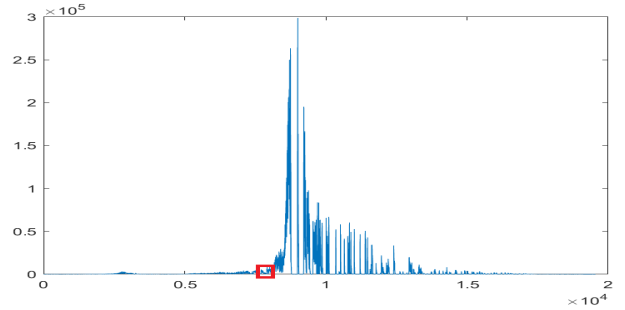


Fig. 6: The evolution of  $e_k$  as a function of  $k$  for  $\delta = 10^8$  and  $\mathbf{b}_0 = \mathbf{0}_{|\mathcal{A}|}$ .

grid comprises 810 buses, 8 substations, and 1 generator, as illustrated in Figure 5. The total active and reactive loads are 5.1267 MW and 0.51 MVar respectively with voltage magnitude  $V_0 = 20$  kV.

The results of these experiments are detailed in Table IV. The optimality gap is calculated as:

$$\text{Gap} = \left( \frac{\text{ADMM losses}}{\text{SRD losses}} - 1 \right) \times 100\%,$$

which provides a measure of the relative difference between the losses computed by Algorithm 1 and the optimal losses established by SRD. The "ADMM losses" represent the values obtained from Algorithm 1, and the "SRD losses" represent the optimal solution values from SRD. It's important to note that due to the simplifications in our model, the losses derived serve as approximations rather than exact values.

Table IV presents results for different values of the parameter  $\delta$ , illustrating the average optimality gap, the range of gap values, and the average iterations required for convergence. The average is computed for Algorithm 1 across 10 restarts, each utilizing a distinct initial state  $\mathbf{b}_0$ .

TABLE IV: Results of execution of Algorithm 1 on the SRD network with different values of  $\delta$ .

$\delta$	Avr. Gap	Min-Max. Gap (kw)	Avg. No. of Iter
1	24.316%	15.29% – 34.67%	19551
10	34.85%	17.43% – 39.86%	15298
100	39.4%	27.12% – 54.76%	12737
$10^8$	54.02%	43.61% – 70.43%	9874

An increase in  $\delta$  corresponds to a notable reduction in iterations, suggesting faster convergence. However, this acceleration comes at the cost of the solution quality, measured by the optimality gap, which diminishes as a trade-off.

We further test the resilience of our algorithm in response to real-time faults in the network. For  $\delta = 10^8$  and  $\mathbf{b}_0 = \mathbf{0}_{|A|}$ , Algorithm 1 took 8698 iteration to converge. A fault is introduced at iteration 8500 by deactivating a line. Figure 6 illustrates the evolution of  $e_k$ , demonstrating that our algorithm successfully adapts to the fault and continues the convergence process. In this scenario, convergence required  $2 \times 10^4$  iterations.

## V. CONCLUSION

This paper introduces a distributed algorithm designed to address the reconfiguration problem in PDNR, characterized by a nonlinear mixed-integer nature without straightforward solutions, especially in distributed environments. To tackle this, we leverage the Alternating Direction Method of Multipliers (ADMM), which breaks down the problem into two simpler sub-problems. Each agent is then tasked with solving a linearly constrained quadratic problem and an MWRAP with locally assigned weights. Extensive numerical experiments have thoroughly showcased the effectiveness and robustness of the proposed algorithm. These experiments provide strong evidence of its efficiency and capability to address real-world problems.

## ACKNOWLEDGMENTS

This work was supported by the National Agency of Research (NAR) through the aLIENOR LabCom program ANR-19-LCV2-0006.

## REFERENCES

- [1] H. Saboori, R. Hemmati, and M. A. Jirdehi, "Reliability improvement in radial electrical distribution network by optimal planning of energy storage systems," *Energy*, vol. 93, pp. 2299–2312, 2015.
- [2] A. Merlin and H. Back, "Search for a minimum-loss operating spanning tree configuration for an urban power distribution system," *Proc of 5th PSCC, 1975*, vol. 1, pp. 1–18, 1975.
- [3] S. Civanlar, J. Grainger, H. Yin, and S. Lee, "Distribution feeder reconfiguration for loss reduction," *IEEE Transactions on Power Delivery*, vol. 3, no. 3, pp. 1217–1223, 1988.
- [4] M. E. Baran and F. F. Wu, "Network reconfiguration in distribution systems for loss reduction and load balancing," *IEEE Power Engineering Review*, vol. 9, no. 4, pp. 101–102, 1989.
- [5] C. Ababei and R. Kavasseri, "Efficient network reconfiguration using minimum cost maximum flow-based branch exchanges and random walks-based loss estimations," *IEEE Transactions on Power Systems*, vol. 26, no. 1, pp. 30–37, 2010.
- [6] Y.-J. Jeon, J.-C. Kim, J.-O. Kim, J.-R. Shin, and K. Y. Lee, "An efficient simulated annealing algorithm for network reconfiguration in large-scale distribution systems," *IEEE Transactions on Power Delivery*, vol. 17, no. 4, pp. 1070–1078, 2002.

- [7] C. Wang and H. Z. Cheng, "Optimization of network configuration in large distribution systems using plant growth simulation algorithm," *IEEE Transactions on Power Systems*, vol. 23, no. 1, pp. 119–126, 2008.
- [8] R. S. Rao, S. V. L. Narasimham, M. R. Raju, and A. S. Rao, "Optimal network reconfiguration of large-scale distribution system using harmony search algorithm," *IEEE Transactions on Power Systems*, vol. 26, no. 3, pp. 1080–1088, 2010.
- [9] H. Khodr, J. Martinez-Crespo, M. Matos, and J. Pereira, "Distribution systems reconfiguration based on opf using Benders decomposition," *IEEE Transactions on Power Delivery*, vol. 24, no. 4, pp. 2166–2176, 2009.
- [10] J. A. Taylor and F. S. Hover, "Convex models of distribution system reconfiguration," *IEEE Transactions on Power Systems*, vol. 27, no. 3, pp. 1407–1413, 2012.
- [11] R. A. Jabr, R. Singh, and B. C. Pal, "Minimum loss network reconfiguration using mixed-integer convex programming," *IEEE Transactions on Power Systems*, vol. 27, no. 2, pp. 1106–1115, 2012.
- [12] S. Mishra, D. Das, and S. Paul, "A comprehensive review on power distribution network reconfiguration," *Energy Systems*, vol. 8, pp. 227–284, 2017.
- [13] D. K. Molzahn, F. Dörfler, H. Sandberg, S. H. Low, S. Chakrabarti, R. Baldick, and J. Lavaei, "A survey of distributed optimization and control algorithms for electric power systems," *IEEE Transactions on Smart Grid*, vol. 8, no. 6, pp. 2941–2962, 2017.
- [14] T. Nagata and H. Sasaki, "A multi-agent approach to power system restoration," *IEEE Transactions on Power Systems*, vol. 17, no. 2, pp. 457–462, 2002.
- [15] A. Elmitwally, M. Elsaid, M. Elgamal, and Z. Chen, "A fuzzy-multiagent service restoration scheme for distribution system with distributed generation," *IEEE Transactions on Sustainable Energy*, vol. 6, no. 3, pp. 810–821, 2015.
- [16] W. Li, Y. Li, C. Chen, Y. Tan, Y. Cao, M. Zhang, Y. Peng, and S. Chen, "A full decentralized multi-agent service restoration for distribution network with dgs," *IEEE Transactions on Smart Grid*, vol. 11, no. 2, pp. 1100–1111, 2019.
- [17] F. Shen, J. C. Lopez, Q. Wu, M. J. Rider, T. Lu, and N. D. Hatzigiorgiou, "Distributed self-healing scheme for unbalanced electrical distribution systems based on alternating direction method of multipliers," *IEEE Transactions on Power Systems*, vol. 35, no. 3, pp. 2190–2199, 2019.
- [18] R. R. Nejad and W. Sun, "Enhancing active distribution systems resilience by fully distributed self-healing strategy," *IEEE Transactions on Smart Grid*, vol. 13, no. 2, pp. 1023–1034, 2021.
- [19] J. C. López, E. M. Gerards, J. L. Hurink, and M. J. Rider, "Enhanced distributed self-healing system for electrical distribution networks using admm," in *2023 IEEE Power & Energy Society General Meeting (PESGM)*. IEEE, 2023, pp. 1–5.
- [20] S. Boyd, N. Parikh, E. Chu, B. Peleato, and J. Eckstein, "Distributed optimization and statistical learning via the alternating direction method of multipliers," *Foundations and Trends® in Machine Learning*, vol. 3, no. 1, pp. 1–122, 2011. [Online]. Available: <http://dx.doi.org/10.1561/22000000016>
- [21] J. Eckstein and W. Yao, "Understanding the convergence of the alternating direction method of multipliers: Theoretical and computational perspectives," *Pac. J. Optim.*, vol. 11, no. 4, pp. 619–644, 2015.
- [22] S. Diamond, R. Takapoui, and S. Boyd, "A general system for heuristic minimization of convex functions over non-convex sets," *Optimization Methods and Software*, vol. 33, no. 1, pp. 165–193, 2018.
- [23] R. Takapoui, N. Moehle, S. Boyd, and A. Bemporad, "A simple effective heuristic for embedded mixed-integer quadratic programming," *International journal of control*, vol. 93, no. 1, pp. 2–12, 2020.
- [24] Q. Peng and S. H. Low, "Distributed algorithm for optimal power flow on a radial network," in *53rd IEEE Conference on decision and control*. IEEE, 2014, pp. 167–172.
- [25] S. Magnússon, P. C. Weeraddana, and C. Fischione, "A distributed approach for the optimal power-flow problem based on admm and sequential convex approximations," *IEEE Transactions on Control of Network Systems*, vol. 2, no. 3, pp. 238–253, 2015.
- [26] T.-L. Nguyen, Q.-T. Tran, R. Caire, Y. Wang, Y. Besanger, and N.-A. Luu, "Distributed optimal power flow and the multi-agent system for the realization in cyber-physical system," *Electric Power Systems Research*, vol. 192, p. 107007, 2021.
- [27] T. Mühlpfordt, X. Dai, A. Engelmann, and V. Hagenmeyer, "Distributed power flow and distributed optimization—formulation, solution, and open source implementation," *Sustainable Energy, Grids and Networks*, vol. 26, p. 100471, 2021.
- [28] B. Korte and J. Vygen, *Combinatorial optimization*, 6th ed., ser. Algorithms and Combinatorics. Springer, 2018, vol. 21.

- [29] H. Ahmadi and J. R. Martí, "Minimum-loss network reconfiguration: A minimum spanning tree problem," *Sustainable Energy, Grids and Networks*, vol. 1, pp. 1–9, 2015.
- [30] B. Stojanović, T. Rajić, and D. Šošić, "Distribution network reconfiguration and reactive power compensation using a hybrid simulated annealing–minimum spanning tree algorithm," *International Journal of Electrical Power & Energy Systems*, vol. 147, p. 108829, 2023.
- [31] A. Cárcamo-Gallardo, L. García-Santander, and J. E. Pezoa, "Greedy reconfiguration algorithms for medium-voltage distribution networks," *IEEE Transactions on Power Delivery*, vol. 24, no. 1, pp. 328–337, 2008.
- [32] M. Guimaraes, C. Castro, and R. Romero, "Distribution systems operation optimisation through reconfiguration and capacitor allocation by a dedicated genetic algorithm," *IET Generation, Transmission & Distribution*, vol. 4, no. 11, pp. 1213–1222, 2010.
- [33] E. M. Carreno, R. Romero, and A. Padilha-Feltrin, "An efficient codification to solve distribution network reconfiguration for loss reduction problem," *IEEE Transactions on Power Systems*, vol. 23, no. 4, pp. 1542–1551, 2008.
- [34] Y. Wang, Y. Xu, J. Li, J. He, and X. Wang, "On the radiality constraints for distribution system restoration and reconfiguration problems," *IEEE Transactions on Power Systems*, vol. 35, no. 4, pp. 3294–3296, 2020.
- [35] S. Lei, C. Chen, Y. Song, and Y. Hou, "Radiality constraints for resilient reconfiguration of distribution systems: Formulation and application to microgrid formation," *IEEE Transactions on Smart Grid*, vol. 11, no. 5, pp. 3944–3956, 2020.
- [36] R. R. Nejad and W. Sun, "Distributed load restoration in unbalanced active distribution systems," *IEEE Transactions on Smart Grid*, vol. 10, no. 5, pp. 5759–5769, 2019.
- [37] A. Choudhary, "Implementation of Edmond's algorithm," 2023, <https://www.mathworks.com/matlabcentral/fileexchange/24899-edmonds-algorithm>, MATLAB Central File Exchange.